Observational study *Clin Ter 2023; 174 (1):61-66* *doi: 10.7417/CT.2023.2498*

Susceptibility of *Bacillus subtilis* to Zinc Oxide Nanoparticles Treatment

S. Djearamane[1]*, A. Sundaraji[1], P. T. Eng[1], S. X. T. Liang[1], L. S. Wong[2], B. Senthilkumar[3]

[1]Department of Biomedical Science, Faculty of Science, Universiti Tunku Abdul Rahman, Kampar, Perak, Malaysia; [2]Department of Biotechnology, Faculty of Health and Life Sciences, INTI International University, Nilai, Negeri Sembilan, Malaysia; [3]Department of Zoology, Thiruvalluvar University, Vellore, Tamil Nadu, India

Abstract

Aim. With the characteristics such as low toxicity, high total surface, ability to inhibit the growth of pathogenic microorganisms, zinc oxide nanoparticles (ZnO NPs), as one of the metallic nanoparticles, have been chosen as an antibacterial agent to treat various skin infections. The present study was aimed to determine the antibacterial potential of ZnO NPs on *Bacillus subtilis*, the Gram-positive bacterium that can cause skin and wound infections.

Methods. *B. subtilis* was exposed to 5 to 150 µg/mL of ZnO NPs for 24 h. The parameters employed to evaluate the antimicrobial potential of ZnO NPs were the growth inhibitory effect on *B. subtilis*, the surface interaction of ZnO NPs on the bacterial cell wall, and also the morphological alterations in *B. subtilis* induced by ZnO NPs.-

Results. The results demonstrated a significant ($p < 0.05$) inhibition of ZnO NPs on *B. subtilis* growth and it was in a dose-dependent manner for all the tested concentrations of ZnO NPs from 5 to 150 µg/mL at 24 h. Fourier transformed infrared (FTIR) spectrum confirmed the involvement of polysaccharides and polypeptides of bacterial cell wall in surface binding of ZnO NPs on bacteria. The scanning electron microscopy (SEM) was used to visualize the morphological changes B. subtilis illustrated several surface alterations such as distortion of cell membrane, roughening of cell surface, aggregation and bending of cells, as well as, the cell rupture upon interacting with ZnO NPs for 24 h.

Conclusion. The results indicated the potential of ZnO NPs to be used as an antibacterial agent against *B. subtilis*. The findings of the present study might bring insights to incorporate ZnO NPs as an antibacterial agent in the topical applications against the infections caused by *B. subtilis*. ***Clin Ter 2023; 174 (1):61-66 doi: 10.7417/CT.2023.2498***

Key words: *Antibacterial activity, Bacillus subtilis, growth inhibition, zinc oxide nanoparticles*

Introduction

Nanotechnology has been widely utilized in various fields, such as food industry, consumer products and medical applications (1). Nanoparticles (NPs) act as carriers for antibiotics with promising results on tackling the pathogen themselves (2). The application of NPs has become an alternative to conventional therapies in treating infections caused by the multidrug resistant and intracellular pathogens. Examples of NPs with bactericidal properties are CuO NPs, TiO_2 NPs, Au NPs, ZnO NPs and Fe_3O_2 NPs (3-5).

ZnO NPs are popularly utilized in biomedical applications including drug delivery, antibacterial, anti-inflammation, anticancer treatment, wound healing, and bio-imaging (6-8) due to the unique properties such as antibacterial, antifungal, UV filtering, anticorrosive and most importantly, low toxicity to humans (9, 10).

Bacillus subtilis is a motile, rod-shaped, non-encapsulated Gram positive bacterium (11). The bacterium form endospore and thus can remain dormancy, it can survive in a diverse environment (12-14) as well as against stress condition (15).

Generally, *B. subtilis* is not pathogenic to humans (16). However, previous studies have reported that *B. subtilis* were accounted for food poisoning (17), bacteraemia in immunocompromised individuals (18), and dermatitis (19). Researchers have reported the detection of *B. subtilis* from multiple surgical wound-drainage sites, wound of a burn patient and breast prosthesis (11, 20, 21). Since most of the reported cases happened after secondary infection, *B. subtilis* was known as an opportunistic pathogen that can lead to nosocomial infection (11, 22). As the nosocomial infection by *B. subtilis* can progress into a serious concern to the public, it requires an urgent medical attention to curb the antibiotic resistance due to nosocomial infections (11).

Due to the proven advantage such as profound antimicrobial activity and low toxicity to human, ZnO NPs can be used as an antibacterial agent in wound dresser or wound batch (23). Hence, the present study investigated the antibacterial effects of ZnO NPs on *B. subtilis* through assessing the growth inhibitory effect, interaction of ZnO NPs on bacterial surface and the subsequent morphological damages caused by ZnO NPs. The findings of this study bring supportive insights to incorporate ZnO NPs as an antibacterial agent in topical applications and wound dressings to curb the infections caused by *B. subtilis*.

Correspondence: *Sinouvassane Djearamane, email: sinouvassane@utar.edu.my; biochsinouvas07@gmail.com

ISSN 1972-6007

Materials and Methods

Characterization of ZnO NPs

Zinc oxide nano-powder with the particle size <100 nm was purchased from Sigma-Aldrich, Malaysia. The size and structure of the nanoparticle were determined using a scanning electron microscope (JSM-6701F, JOEL, Japan), operated at an acceleration voltage of 4 kV with a working distance of 4.7 mm. In addition, the energy dispersive X-ray (EDX) spectrum was used to confirm the chemical composition of ZnO NPs.

Preparation of ZnO NPs stock solution

The stock solution of ZnO NPs (300 µg/mL) was prepared by dissolving a 9 mg of ZnO NPs powder in a 30 mL of Luria-Bertani broth (LB broth) followed by ultrasonication for 30 min at 37 kHz to make the solution homogenous. The solution was diluted with LB broth to yield the following working concentrations, 5 µg/mL (1:60 dilution), 10 µg/mL (1:30 dilution), 25 µg/mL (1:12 dilution), 50 µg/mL (1:6 dilution), 100 µg/mL (1:3 dilution) and 150 µg/mL (1:2 dilution).

Bacterial Growth Curve

The bacterium *B. subtilis* was cultured in Luria-Bertani broth (LB broth) in a 15 mL falcon tube at 37 °C. The growth rate of *B. subtilis* was measured through the turbidity reading of the culture suspension at 600 nm using UV spectrophotometer (Implen, C40, Germany) at a range of time intervals, 0, 2 4, 6, 8, 24 and 48 h. A growth curve was then constructed from the readings to determine the mid-log phase.

Exposure of Bacteria to ZnO NPs

The six different working concentrations of ZnO NPs (5, 10, 25, 50, 100 and 150 µg/mL) were prepared by diluting the ZnO NPs stock solution using LB broth. A 5 ml of bacteria suspension that was incubated to mid-log phase for 4 h with an initial OD_{600} of 0.05 was exposed to 5, 10, 25, 50, 100 and 150 µg/mL of ZnO NPs in 15 mL falcon tube and incubated for 24 h at 37°C without shaking. Bacteria culture without the addition of ZnO NPs was treated as the negative control, while the bacteria culture treated with antibiotic Ciprofloxacin (500 µg/mL) was considered as a positive control.

Investigation of Bacterial Growth Inhibition

Turbidity method was employed to examine the bacteriostatic effect of ZnO NPs. The turbidity of the ZnO NPs-treated bacterial suspensions as well as the negative and positive controls were measured using UV-vis spectrophotometer (Implen, C40, Germany) at OD_{600}. The OD_{600} of ZnO NPs suspension for each concentration was measured and subtracted from the test reading to eliminate the interference from NPs. The percentage of inhibition in the bacterial growth after 24 h of exposure to ZnO NPs was evaluated by using the equation below:

$$\text{Percentage of growth inhibition} = \frac{OD_{control} - OD_{test}}{OD_{control}} \times 100\%$$

Interaction of ZnO NPs on Bacterial Cell Wall

The FTIR spectroscopy was performed to identify the involvement of the biomolecules from the bacterial cell wall in binding of ZnO NPs on bacteria. A volume of 5 mL of bacteria cell suspension was treated with 150 µg/mL ZnO NPs for 24 h along with negative control (untreated bacterial suspension) were centrifuged for 10 min at 6000 *g*. The pellet was washed with 1X PBS for three times and freeze-dried. Then the freeze dried bacteria powder was subjected to FTIR (FTIR, Nicoler IS 10, United States of America) analysis over the range of 4000 to 400 cm^{-1}.

Scanning electron microscopy

The scanning electron microscope (SEM, JSM-6701F, JOEL, Japan) was chosen to view the morphological changes induced on *B. subtilis* upon treating with ZnO NPs for 24 h. A 15 ml volume of the negative control and 150 µg/mL ZnO NPs treated bacterial suspension were centrifuged for 10 min at 6000 *g*. The pellet was washed with 1X PBS followed by fixation with 2.5 % glutaraldehyde for overnight. The pellet was then dehydrated with a series of ethanol at the following concentration 50%, 75%, 95% and 100%. The pellets then were freeze-dried and subjected to scanning electron microscopy.

Statistical Analysis

Statistical analysis was performed to analyse the variance induced by six distinct concentrations of ZnO NPs on the bacteria cells interacted with ZnO NPs for 24 h. The experiments were done in triplicates (n=3) and the data are presented as mean ± standard deviation.

Results and Discussion

Characterization of ZnO NPs

The SEM observation of ZnO nanopowder confirmed mixture of rod and spherical shaped particles with an average size of 49.85 nm (Fig. 1(A). EDX analysis confirmed the presence of zinc and oxygen in the ZnO NPs powder (Fig. 1(B).

Growth Curve of Bacterium

The growth pattern of *B. subtilis* was determined by plotting the growth curve as shown in Figure 2. The bacterial cells were in the lag phase from 0 to 2 h, the log phase of *B. subtilis* was started at 2 h and lasted until 7 h, and the mid-log phase was identified at 4 h. The growth of *B. subtilis* declined from 24 to 48 h. During the lag phase the growth will be slow as the bacteria take time to adapt to the medium (24). According to Rolfe et al. (2011) (25), each individual cells will increase in size only, not the cell number despite there are ample nutrients available. During the log phase, the bacteria begins to divide actively by binary fission (26) and attain their maximal growth rate. The stationary phase usually occur at 18 h to 24 h where the waste products start

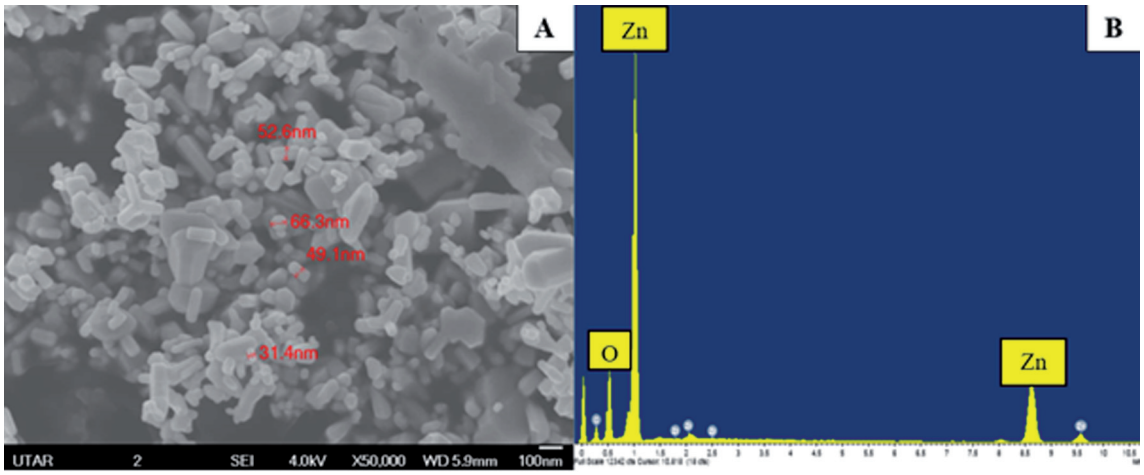

Fig. 1. Characterisation of ZnO NPs under (A) SEM with 50,000X magnification and (B) EDX spectrum showing the presence of zinc and oxygen in ZnO NPs powder.

to pile up and the nutrients begin to deplete (26, 27). After 24 h, the bacterial population steps into the death phase where they drop cell-division ability and the number of live cells reduce (26). In the present study, the bacteria cells were exposed to ZnO NPs at the mid-log phase (4 h) as the cells are most active in terms of metabolism and multiplication at their mid-exponential phase (24, 28).

Growth Inhibition Test

The results confirmed a significant ($p < 0.05$) inhibition of ZnO NPs on *B. subtilis* growth and it was in a dose-dependent manner for all the tested concentrations of ZnO NPs from 5 to 150 µg/mL at 24 h. The percentage of growth inhibition for 5, 10, 25, 50, 100, 150 µg/mL were reported to be 11.88 ± 0.04, 16.66 ± 0.80, 28.55 ± 0.36, 33.57 ± 0.38, 47.52 ± 1.53, 70.09 ± 1.5%, respectively (Fig. 3). Meanwhile, the positive control showed 92.96 ± 0.19% of inhibition. Further, the results were observed to be dose dependant as the percentage of growth inhibition of B. subtilis increased with the increasing concentrations of ZnO NPs.

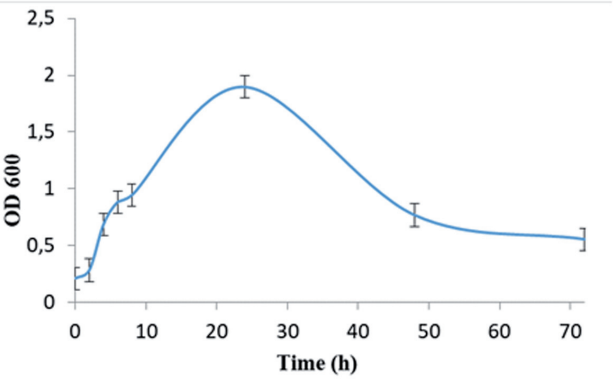

Fig. 2. Growth curve of B. subtilis in Luria-Bertani broth (LB broth) at 37°C

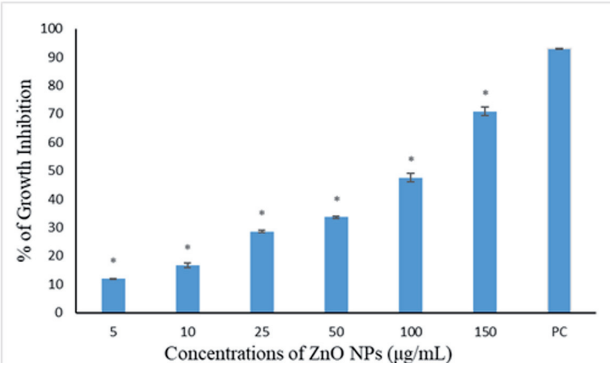

Fig. 3. Percentage of growth inhibition by turbidity method on *B. subtilis* upon treatment with different concentrations of ZnO NPs for 24 h at 37°C in Luria-Bertani broth. * indicates the significant difference between negative control and the bacterial suspensions treated with different concentrations of ZnO NPs at $p<0.05$.

Previous studies reported similar findings on the growth inhibition effects of ZnO NPs on bacteria. Jones et al. (29) reported a dose-dependent growth inhibition on Gram positive bacteria, *B. subtilis, Staphylococcus aureus, Staphylococcus epidermidis* and *Enterococcus faecalis* with increasing concentration of ZnO NPs. The highest percentage of growth inhibition on all the tested bacteria was reported to be 95% at 400 µg/mL ZnO NPs for 10 h of treatment. Singh and Nanda (30) revealed a dose dependant growth inhibition of ZnO NPs on *Aspergillus niger* for 12.5 to 50 µg/mL of ZnO NPs at 24 h.

Besides, a study on both Gram positive and Gram negative bacteria such as *B. subtilis, Streptococcus pyogenes, E. faecalis, Bacillus cereus, Proteus vulgaris, Escherichia coli, Pseudomonas alcaligenes, Enterobacter aerogenes*, and *Shigella flexneri* reported 95% of growth inhibition when exposed to 320 to 560 µg/mL of ZnO NPs at 8 h (31). Azizi-Lalabadi et al. (32) illustrated the antibacterial properties of ZnO and TiO_2 nanomaterials with zeolite against *Listeria monocytogenes, S.aureus, Escherichia coli*

O157:H7 and *Pseudomonas fluorescens.* While Qiu et al. (2020) (33) showed the antibacterial effect of calcinied ZnO NPs and CuO NPs under the exposure of UV on *E. coli* and *S. aureus.* Meanwhile, Nilavukkarasi et al. (34), demonstrated the intense antibacterial effects of ZnO NPs synthesised from the leaves C*apparis zeylanica* on the tested microorganisms included *S. epidermidis, E. faecalis, Shigella dysenteriae, Candida albicans, Aspergillus niger* and *Salmonella paratyphi.*

Surface Interaction of ZnO NPs on Bacterial Cell Wall

FTIR analysis was aimed to examine the functional groups of bacterial cell surface that were involved in surface interaction of ZnO NPs on bacterial cell wall. It was done by comparing the peaks between the negative control and bacterial suspension treated with 150 µg/mL ZnO NPs for 24 h. Based on Fig. 4, the negative control demonstrated O-H and N-H stretching at 3447 cm^{-1}, C-H stretching at 2373 and 2345 cm^{-1}, C=O stretching at 1639 cm^{-1}, carbon moieties at 556 cm^{-1}. Meanwhile, the spectrum of ZnO NPs treated bacterial suspension showed O-H and N-H stretching (3447 to 3436 cm^{-1}), C-N stretching of an amine group (2373 to 2370 cm^{-1}), C=O stretching (1639 to 1637 cm^{-1}), Zn-O stretching (556 to 582 cm^{-1}). According to Melin et al. (35) and Gorgulu et al. (36), the regions between 3447 cm^{-1} and 3325 cm^{-1} were dominated by the O-H and N-H stretching vibration from proteins and polysaccharides. The shift of peak from 2373 cm^{-1} to 2370 cm^{-1} was dominated by the C-N stretching from the polypeptides (37). Further, the shifting of the peak from 1639 cm^{-1} to 1637 cm^{-1}, corresponded with C=O stretching of the polypeptide and protein backbone (38). The last shifting of the peak, from 556 cm^{-1} to 582 cm^{-1}, corresponded to glycogen (38). Nevertheless, Arshad et al. (39) also correlated this region to the Zn-O bond. Overall, FTIR spectrum confirmed the involvement of polysaccharides and polypeptides of bacterial cell wall in surface binding of ZnO NPs on bacterial cell surface (Table 1).

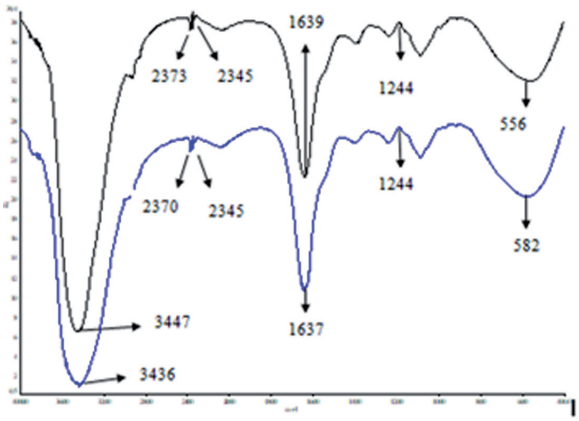

Fig. 4. FTIR spectrum of (A) negative control (black) and (B) 150 µg/mL ZnO NPs treated *B. subtilis* (blue).

Table 1. Possible involvement of biomolecules from bacterial cell wall in surface binding of ZnO NPs on bacteria by FTIR analysis

Absorption (cm^{-1})	Molecular motion	Functional group	Biomolecules
3447 →→ 3436	O-H and N-H stretching	Alcohol, amide A	Proteins, polysaccharides
2373 →→ 2370	C-H stretching	Alkenes	Hydrocarbon
1639 →→ 1637	C=O stretching,	Amide I	Polypeptide, protein backbone
556 →→ 582	Zn-O stretching	Zinc oxide	Glycogen

Alterations in Bacterial Morphology

"The scanning electron microscopy (SEM) was used to visualize the morphological changes in *B. subtilis*, illustrated several surface alterations such as distortion of cell membrane, roughening of cell surface, aggregation and bending of cells, as well as the cell rupture upon interacting with ZnO NPs for 24 h (Fig. 5). Similar findings were reported on *E. coli* (40, 41), *Bacillus cereus* (42), *Chlorella vulgaris* (43) after treating with different types of metallic NPs. According to Djearamane et al. (44), changes in morphology, particularly the aggregation of the cells was aimed to promote self-defence and thus lesser total surface area could be engaged for ZnO NPs to bind. The successful accumulation of NPs on the cell surface affects the cell wall integrity and also may lead to their uptake into the cell (43).

The antibacterial effect of ZnO NPs begins after the NPs attach to the surface of the bacterial cell wall (45). Liu et al. (46) proposed that Zn^{2+} ions leach out when the NPs are mixed with the LB medium before the attachment. The subsequent interaction which involves the binding of the positively charged Zn^{2+} ion with both the –SH bonds in the cellular protein and the negatively charged functional groups of macromolecules (47, 48) will result in a series of physiological changes, such as disintegration of membrane, malfunction of cellular protein and genomic instability (2, 49, 50, 51). In addition, the mass production of reactive oxygen species (ROS) such as superoxide anion and hydrogen peroxide (41) results from the interaction of ZnO NPs constitutes the main reason for growth inhibition. Nevertheless, the bacterial defence mechanism, notably the expression of cytosolic protein and reductase (52) surge up to wipe out the ROS generated. However, when the amount of ROS exceeds the antioxidant enzymes, it will result in cell death (53).

Conclusion

The results of the present study indicated the potential of ZnO NPs to be used as an antibacterial agent against *B. subtilis*. The findings of the present study might bring insights to incorporate ZnO NPs as an antibacterial agent in the topical applications against the infections caused by *B. subtilis*.

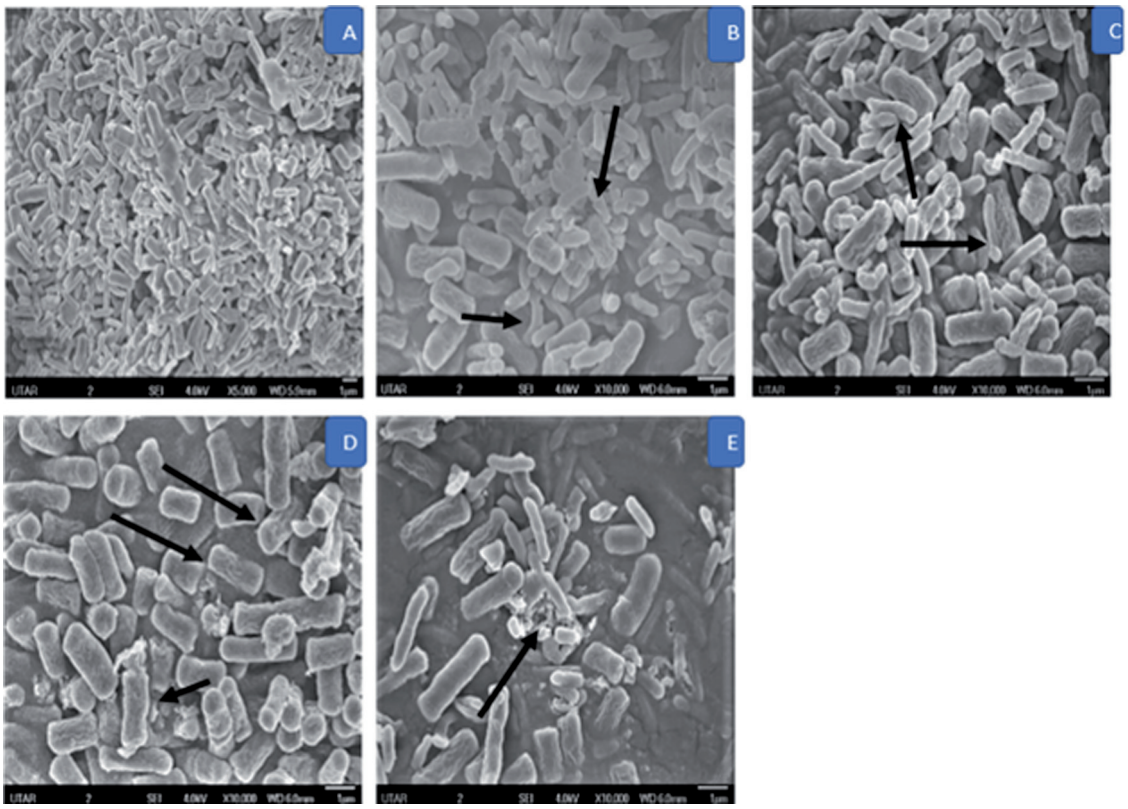

Fig. 5. SEM image of negative control (A) and bacteria treated with 150 µg/mL of ZnO NPs for 24 h showing aggregation and bending of bacterial cells (B); cell membrane distortion (C), deformity and roughening of cell surface (D); cell rupture (E) observed under 10,000X magnification and scale bars are in 1 µm.

References

1. Dhas SP, Shiny PJ, Khan S, et al. Toxic behaviour of silver and zinc oxide nanoparticles on environmental microorganism. Journal of Basic Microbiology, 2014; 53:1-12.
2. Wang L, Hu C, Shao L. The antimicrobial activity of nanoparticles: present situation and prospects for the future. International Journal of Nanomedicine. 2017; 12:1227.
3. Dakal TC, Kumar A, Majumdar RS, et al. Mechanistic Basis of Antimicrobial Actions of Silver Nanoparticles. Frontiers in Microbiology. 2016; 7:1831.
4. Hemeg HA. Nanomaterials for alternative antibacterial therapy. International Journal of Nanomedicine. 2017; 12:8211-8225.
5. Slavin YN, Asnis J, Häfeli UO, et al. Metal nanoparticles: understanding the mechanisms behind antibacterial activity. Journal of Nanobiotechnology. 2017; 15:65.
6. Keefer KA, Iocono JA, Ehrlich HP. Zinc-containing wound dressings encourage autolytic debridement of dermal burns. Wound Repair and Regeneration. 1998; 10:54-58.
7. Xiong HM. ZnO nanoparticles applied to bioimaging and drug delivery. Advanced Materials. 2013; 25:5329–5335.
8. Zhang ZY, Xiong HM. Photoluminescent ZnO nanoparticles and their biological applications. Materials. 2015; 8:3101-3127.
9. Hatamie A, Khan A, Golabi M, et al. Zinc oxide nanostructure-modified textile and its application to biosensing, photocatalysis, and as antibacterial material. Langmuir. 2015; 31:10913–10921.
10. Reddy KM, Feris K, Bell J, et al. Selective toxicity of zinc oxide nanoparticles to prokaryotic and eukaryotic systems. Applied Physics Letters. 2007; 90:213902-1-213902-3.
11. Saleh F, Kheirandish F, Azizi H, et al. Molecular Diagnosis and Characterization of Bacillus subtilis Isolated from Burn Wound in Iran. Research in Molecular Medicine. 2014; 2:40-44.
12. Earl AM, Losick R, Kolter R. Ecology and genomics of Bacillus subtilis. Trends in Microbiology. 2006; 16:269–275.
13. Brown KL. Control of Bacterial Spores. British Medical Bulletin. 2000; 56:158-71.
14. Turnbull P, Quinn C, Henderson I. Bacillus anthracis and Other Bacillus species. Molecular Medical Microbiology. 2002; 2011–2031.
15. Liu PF, Lo CW, Chen CH, et al. Use of nanoparticles as therapy for methicillin-resistant Staphylococcus aureus infections. Current Drug Metabolism. 2009; 10:875-84.
16. Valdez A, Yepiz-Plascencia G, Ricca E, et al. First Litopenaeus vannamei WSSV 100% oral vaccination protection using CotC::Vp26 fusion protein displayed on Bacillus subtilis spores surface. Journal of Applied Microbiology. 2014; 117:347-357.
17. Logan NA. Bacillus species of medical and veterinary importance. Journal of Medical Microbiology. 1988; 25:157–165.
18. Beebe JL, Koneman EW. Recovery of uncommon bacteria from blood: association with neoplastic disease. Clinical Microbiology Reviews. 1995; 8:336–356.

19. Smith DJ, Toby Mathias CG, Greenwald DI. Contact dermatitis from B. subtitlis -derived protease enzymes. Contact Dermatitis. 1989; 20:58–59.
20. Nicolas P, Made, U, Dervyn E, et al. Condition-Dependent Transcriptome Reveals High-Level Regulatory Architecture in Bacillus subtilis. Science. 2012; 335:1103-1106.
21. Oggioni MR, Pozzi G, Valensin PE. Recurrent Septicemia in an Immunocompromised Patient Due to Probiotic Strains of Bacillus subtilis. Journal of Clinical Microbiology. 1998; 36:325-326.
22. Bais HP, Fall R, Vivanco JM. Biocontrol of Bacillus subtilis against infection of Arabidopsis roots by Pseudomonas syringae is facilitated by biofilm formation and surfactin production. Plant Physiology. 2004; 134:307-319.
23. Aloe C, Feltis B, Wright P, et al. Potential for enhanced wound healing with ZnO nanoparticles. Frontiers in Bioengineering and Biotechnology. 2016; 10.
24. Allen RJ, Waclaw B. Microbial population dynamics and evolution: a statistical physicist's guide. Reports on Progress in Physics. 2018; 82.
25. Rolfe MD, Rice CJ, Lucchini S, et al. Lag Phase Is a Distinct Growth Phase That Prepares Bacteria for Exponential Growth and Involves Transient Metal Accumulation. Journal of Bacteriology. 2011; 194:686–701.
26. Wang L, Fan D, Chen W, et al. Bacterial growth, detachment and cell size control on polyethylene terephthalate surfaces. Scientific Reports. 2015; 5.
27. Kolter R, Siegele DA, Tormo A. The Stationary Phase of The Bacterial Life Cycle. Annual Review of Microbiology. 1993; 47:855–874.
28. Dadi R, Rabah A, Traore M, et al. Antibacterial activity of ZnO and CuO nanoparticles against Gram positive and Gram negative strains. Materials Science and Engineering: C. 2019; 104:109968.
29. Jones N, Ray B, Ranjit KT, et al. Antibacterial activity of ZnO nanoparticle suspensions on a broad spectrum of microorganisms. FEMS Microbiology Letters. 2008; 279:71–76.
30. Singh P, Nanda A. Antimicrobial and antifungal potential of zinc oxide nanoparticles in comparison to conventional zinc oxide particles. Journal of Chemical and Pharmaceutical Research. 2013; 5:457-463.
31. Raghupathi KR, Koodali RT, Manna AC. Size-dependent bacterial growth inhibition and mechanism of antibacterial activity of zinc oxide nanoparticles. Langmuir. 2011; 27:4020-4028.
32. Azizi-Lalabadi M, Ehsani A, Divband B, et al. Antimicrobial activity of Titanium dioxide and Zinc oxide nanoparticles supported in 4A zeolite and evaluation the morphological characteristic. Scientific Reports. 2019; 9.
33. Qiu S, Zhou H, Shen Z, et al. Synthesis, characterization, and comparison of antibacterial effects and elucidating the mechanism of ZnO, CuO and CuZnO nanoparticles supported on mesoporous silica SBA-3. Royal Society of Chemistry Advances. 2020; 10:2767–2785.
34. Nilavukkarasi M, Vijayakumar S, Prathipkumar S. Capparis zeylanica mediated bio-synthesized ZnO nanoparticles as antimicrobial, photocatalytic and anti-cancer applications. Materials Science for Energy Technologies. 2020.
35. Melin A, Peromat A, Deleris G. Pharmacologic application of Fourier transform IR spectroscopy: In vivo toxicity of carbon tetrachloride on rat liver. Biopolymers (Biospectroscopy). 2000; 57:160-168.
36. Gorgulu ST, Dogan M, Severcan F. The characterization and differentiation of higher plants by Fourier transform infrared spectroscopy. Applied Spectroscopy. 2007; 61:300-308.
37. Ahluwalia SS, Goyal D. Removal of heavy metals by waste tea leaves from aqueous solution. Engineering in Life Sciences. 2005; 5:158-162.
38. Garip S, Gozen AC, Severcan F. Use of Fourier transform infrared spectroscopy for rapid comparative analysis of Bacillus and Micrococcus isolates. Food Chemistry. 2009; 113:1301-1307.
39. Arshad M, Farrukh MA, Imtiaz A, et al. Solvent assisted synthesis of tin-zinc oxide nanoparticles: Structural characterization and antimicrobial activity. Asian Journal of Chemistry. 2015; 27:371-374.
40. Arakha M, Pal S, Samantarrai D, et al. Antimicrobial activity of iron oxide nanoparticle upon modulation of nanoparticle-bacteria interface. Scientific Reports. 2015; 5:1-16.
41. Zhang L, Ding Y, Povey M, et al. ZnO nanofluids – A potential antibacterial agent. Progress in Natural Science. 2008; 18:939–944.
42. Aguilar CAH, Jimenez ABP, Silva AR, et al. Organic-Inorganic Hybrid Nanoparticles for Bacterial Inhibition: Synthesis and Characterization of Doped and Undoped ONPs with Ag/Au NPs. Molecules. 2015; 20:6002-6021.
43. Djearamane S, Wong LS, Mooi LY, et al. Short-term cytotoxicity of zinc oxide nanoparticles on Chlorella vulgaris. Sains Malaysiana. 2019; 48:69-73.
44. Djearamane S, Wong LS, Mooi LY, et al. Cytotoxic effects of zinc oxide nanoparticles on cyanobacterium Spirulina (Arthrospira) platensis. PeerJ. 2018; 6:4682.
45. Dwivedi S, Wahab R, Khan F, et al. Reactive Oxygen Species Mediated Bacterial Biofilm Inhibition via Zinc Oxide Nanoparticles and Their Statistical Determination. PLoS ONE. 2014; 9:e111289.
46. Liu S, Killen E, Lim M, et al. The effect of common bacterial growth media on zinc oxide thin films: identification of reaction products and implications for the toxicology of ZnO. Royal Society of Chemistry Advances. 2014; 4:4363–4370.
47. Padmavathy N, Vijayaraghavan R. Enhanced bioactivity of ZnO nanoparticles—an antimicrobial study. Science and Technology of Advanced Materials. 2008; 9:035004.
48. Dutta RK, Nenavathu BP, Gangishetty MK, et al. Antibacterial effect of chronic exposure of low concentration ZnO nanoparticles on E. coli. Journal of Environmental Science and Health: Part A. 2013; 48:871-878.
49. Jiang Y, Zhang L, Wen D, et al. Role of physical and chemical interactions in the antibacterial behaviour of ZnO nanoparticles against E. coli. Materials Science and Engineering: C. 2016; 69:1361-1366.
50. Shi LE, Li ZH, Zheng W, et al. Synthesis, antibacterial activity, antibacterial mechanism and food applications of ZnO nanoparticles: a review. Food Additives and Contaminants: Part A 2014; 31:173-186.
51. Liang SXT, Wong LS, Lim YM, et al. Effects of Zinc Oxide nanoparticles on Streptococcus pyogenes. South African Journal of Chemical Engineering. 2020; 34:63-71.
52. Hsueh YH, Ke WJ, Hsieh CT, et al. ZnO Nanoparticles Affect Bacillus subtilis Cell Growth and Biofilm Formation. PLOS ONE. 2015; 10:e0128457
53. Wahab R, Mishra A, Yun SI, et al. Antibacterial activity of ZnO nanoparticles prepared via non-hydrolytic solution route. Applied Microbiology Biotechnology. 2010; 87:1917–1925.